Princeton Plasma Physics Laboratory

PPPL-

PPPL-

Princeton Plasma Physics Laboratory
Report Disclaimers

Full Legal Disclaimer

Trademark Disclaimer

PPPL Report Availability

Princeton Plasma Physics Laboratory:

http://www.pppl.gov/techreports.cfm

Office of Scientific and Technical Information (OSTI):

http://www.osti.gov/bridge

Related Links:

U.S. Department of Energy

Office of Scientific and Technical Information

Fusion Links

Fast-ion energy loss during TAE avalanches in the National Spherical Torus Experiment

E. D. Fredrickson, N. A. Crocker[1], D. S. Darrow, N. N. Gorelenkov, G. J. Kramer, S. Kubota[1], M. Podesta, R. B. White, A. Bortolon[2], S. P. Gerhardt, R. E. Bell, A. Diallo, B. LeBlanc, F. M. Levinton[3], H. Yuh[3]

Princeton Plasma Physics Laboratory, Princeton New Jersey 08543
[1]*Univ. of California, Los Angeles, CA 90095*
[2]*Univ. of California., Irvine, CA 92697*
[3]*Nova Photonics, Princeton, NJ 08543*

Strong TAE avalanches on NSTX, the National Spherical Torus Experiment [M. Ono, et al., Nucl. Fusion **40** (2000) 557] are typically correlated with drops in the neutron rate in the range of 5% - 15%. In previous studies of avalanches in L-mode plasmas, these neutron drops were found to be consistent with modeled losses of fast ions. Here we expand the study to TAE avalanches in NSTX H-mode plasmas with improved analysis techniques. At the measured TAE mode amplitudes, simulations with the ORBIT code predict that fast ion losses are negligible. However, the simulations predict that the TAE scatter the fast ions in energy, resulting in a small ($\approx 6\%$) drop in fast ion β. The net decrease in energy of the fast ions is sufficient to account for the bulk of the drop in neutron rate, even in the absence of fast ion losses. This loss of energy from the fast ion population is comparable to the estimated energy lost by damping from the Alfvén wave during the burst. The previously studied TAE avalanches in L-mode are re-evaluated using an improved calculation of the potential fluctuations in the ORBIT code.

I. Introduction

The national spherical torus experiment (NSTX) is a medium size (major radius $\approx$ 0.85m, minor radius $\approx$ 0.65m), low aspect ratio tokamak capable of toroidal fields up to 5.6 kG and plasma currents up to 1.4 MA [1]. The plasma can be heated with up to 6 MW of deuterium neutral beams, which are injected with energies from $\approx$ 65 keV up to 90 keV. At these energies, the beam ion velocities are several times the Alfvén velocity over the typical ranges of plasma density and magnetic field.

The super-Alfvénic fast ion population routinely excites a broad spectrum of MHD and Alfvénic mode activity, extending from low frequency (< 50 kHz) fishbone and other kink-like modes [2-7], Toroidal Alfvén Eigenmodes [8-12], up to Compressional and Global Alfvén

Fig. 1 a) spectrogram of magnetic fluctuations, b) Plasma current and neutral beam power evolution.

modes [13-27] with frequencies up to $\approx$ 2.5 MHz and occasionally at even higher frequencies (Fig. 1a). Similar Alfvénic instabilities have also been extensively studied on the beam-heated START and MAST devices [28-39]. TAE were, of course, discovered in conventional beam and ICRF heated tokamaks [40-49]. Experimental and theoretical efforts are underway to characterize these various modes, understand the mechanisms for excitation of the modes, how apparently disparate modes interact [50,51], and the affect that the multiple modes have on the fast ion population. For example, the TAE avalanches shown here appear to be triggered by avalanches of GAE near 800 kHz [52].

The Toroidal Alfvén Eigenmodes (TAE) in NSTX are seen in a broad range of beam-heated plasma regimes, but most commonly in plasmas with lower density, hence relatively larger fast ion populations (*e.g.*, in equilibrium $\tau_E/\tau_{slow} = \beta_{fast}/\beta_{thermal}$). Typically, H-modes in NSTX are too high density, and the density profile is too flat for reflectometers. Previous simulations of fast ion losses with the ORBIT code for TAE avalanches were done using data from L-mode plasmas [8-12]. The measured mode amplitude was found to be in approximate agreement with the threshold for fast ion losses [53]. In this paper we extend
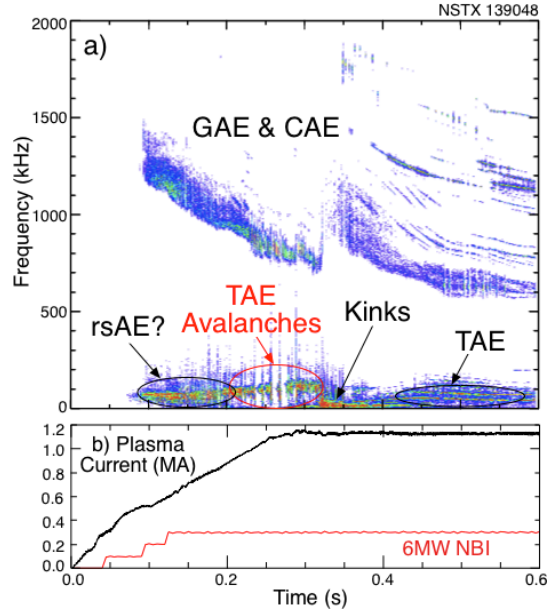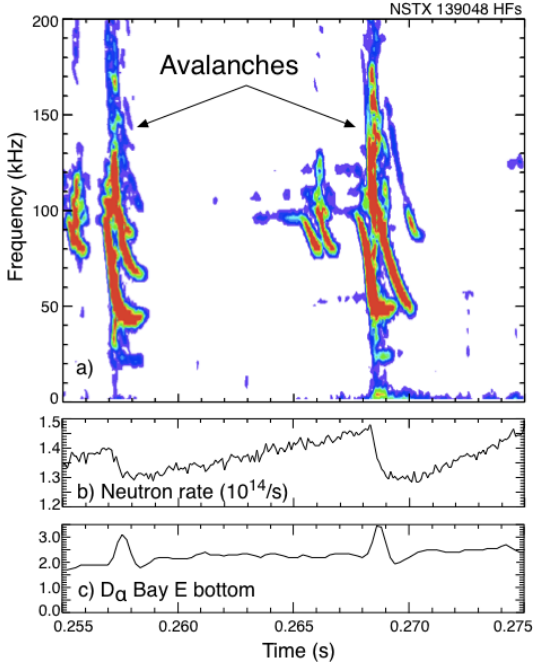
Fig. 2. a) Spectrogram of magnetic fluctuations showing two TAE avalanche bursts, b) neutron rate drops at each burst (note suppressed zero), c) Dα spikes at bursts.

the investigation of TAE mode avalanches to low density H-mode plasmas, and apply the improved analysis techniques to the previously analyzed L-mode TAE avalanches.

In Fig. 1a we show a spectrogram of magnetic fluctuations for a low density H-mode plasma with moderate density peaking where TAE avalanching is present from roughly 0.2 s to 0.35 s. The time history of plasma current and neutral beam power are shown in Fig. 1b. The beams are injected with three sources, each providing 2 MW of deuterium beams at a full-energy of 90 keV. The three beam sources are injected co-tangentially with tangency radii of 0.497 m, 0.592 m and 0.694 m, respectively.

The magnetic fluctuation spectrogram is expanded in Fig. 2a showing TAE avalanches at ≈ 0.259 s and ≈ 0.268 s. As is typical, the TAE occur as a sequence of bursts, with each burst chirping downward in frequency (Fig. 2a). Drops in the neutron rate of 7% and 12% are seen to be correlated with the TAE avalanches in Fig. 2b. The neutron rate ramps up nearly linearly between avalanches, suggesting the next avalanche is triggered before the fast ion population reaches equilibrium. In Fig. 2c, spikes in D-alpha light coincident with the avalanches suggest bursts of lost beam ions are striking PFCs coincident with the neutron rate drops.

In Fig. 3 are shown profiles vs. major radius of some important plasma parameters for this H-mode shot (red) and the previously analyzed L-mode shot
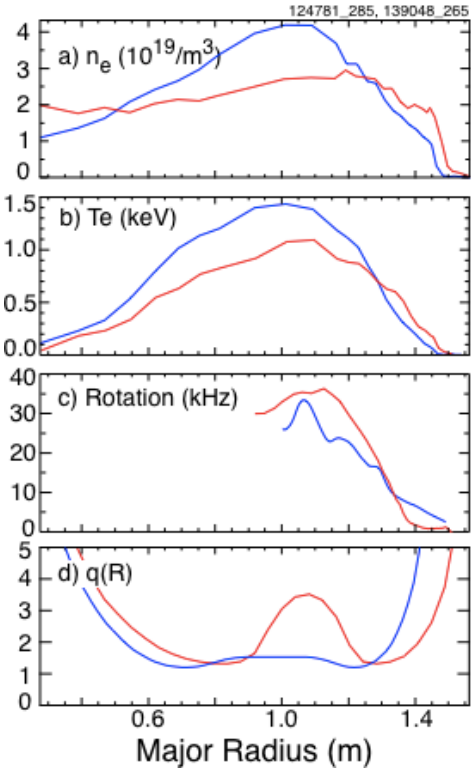

Fig. 3 Profiles of a) density, b) electron temperature, c) rotation velocity and d) q for the H-mode (red) and L-mode (blue).

(blue). The central density is lower and the profile less peaked (Fig. 3a). The electron temperatures are comparable in both shots (Fig. 3b). The broader density profile would change the TAE gap, or continuum, structure, but the gap structure is more strongly affected by the strong sheared toroidal rotation (Fig. 3c), similar in both shots. Both show shear reversal in the q-profile, with the H-mode having stronger shear reversal (Fig. 3d). The q-profiles were reconstructed using Motional Stark Effect measurements of the magnetic field pitch angle [54] and the LRDFIT equilibrium code [55].

The TAE avalanches provide an opportunity to validate codes used for modeling fast ion transport. The process begins with equilibrium reconstruction and TRANSP [56] runs to validate the kinetic data and simulate beam deposition. The TAE are characterized with Mirnov coil arrays which measure the toroidal mode numbers and with a reflectometer array which provides an absolute, internal measurement of the mode amplitude evolution , as well as some information on the radial structure of the modes [57] and the NOVA-k code [58,59] is used to predict the linear growth and damping rates. The ideal, fixed boundary, NOVA code is used to model the eigenmode structures. The NOVA eigenmodes are compared with the reflectometer data to find the best fits to the experimental mode profiles. Those eigenmodes are then imported to the ORBIT code [60], together with the experimentally measured amplitude and frequency evolutions. The ORBIT simulations discussed here were done with 4000 fast ions, representative of the fast-ion slowing-down distribution function calculated in TRANSP.

In this paper we focus primarily on the ORBIT simulations. The analysis of experimental data and the NOVA simulations were discussed in detail previously [53].
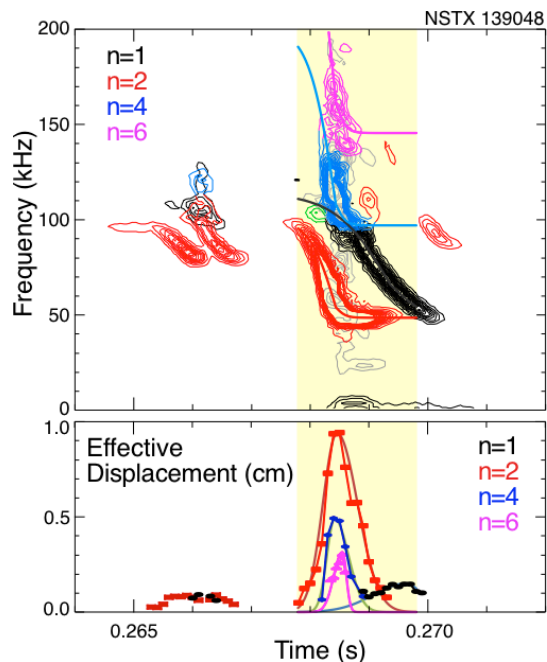

Fig. 4. a) Spectrogram of a Mirnov coil where contours are color-coded to indicate the toroidal mode numbers, as indicated in the legend, b) the peak mode amplitude evolution for each mode from the reflectometer array.

II. TAE avalanches in H-mode plasmas

The modeling of fast ion losses from TAE

avalanches begins with the measurement of the toroidal mode numbers using a toroidal array of Mirnov coils. A spectrogram of a Mirnov coil signal of the avalanche at 0.268 s is shown in Fig. 4a where toroidal mode #'s are indicated by the contour colors. There are four important modes in the final avalanche burst (region indicated in yellow), beginning with the strong growth of an n=2 TAE (red contours). The n=4 and n=6 modes appear strongly coupled to the n = 2 mode in that the frequency evolutions of the n = 4 and 6 modes (blue and magenta contours, respectively) are nearly harmonics of the n = 2 mode. An n=1 TAE appears towards the end of the burst. The amplitude evolution of these four modes as measured with the three innermost reflectometer channels are shown in Fig. 4b. There are two weaker bursts of modes prior to the final avalanche burst. These modes, as is typical, are roughly a factor of ten lower in amplitude.

The linear eigenmodes for each of the four dominant modes in Fig. 4 are calculated with NOVA using the plasma equilibrium as input. Strong, sheared, plasma toroidal rotation greatly affects the structure of the TAE continuum, as seen in Fig. 5. The eigenmodes are calculated with a version of NOVA which includes some of the physics due to the sheared rotation. This is particularly important in low aspect ratio tokamaks where the low field results in a relatively low frequency for the TAE, but strong, co-tangential neutral beam injection spins the plasma at frequencies higher, in some cases, than the TAE frequency. In the gap structure shown in Fig. 5 for the n=2 mode, it is seen that the
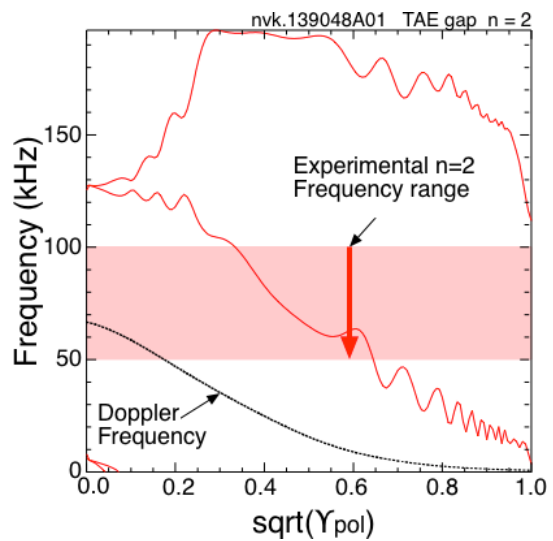
Fig. 5. The continuum structure for the n=2 TAE including the experimental sheared rotation profile. Red band shows range of the n=2 TAE frequency chirp.

TAE frequency at mode onset intersects the continuum, and towards the end of the frequency chirp is of order zero in the plasma frame near the axis. This raises important physics issues concerning the coupling of TAE to MHD modes, such as kinks [50,51]. In practice, it also means that the TAE gap is generally closed on NSTX, that is that the mode stability should not be strongly affected by changes either in the q-profile or the density profile. In fact, quite often the TAE chirp down in frequency from $\approx$100 kHz to $\approx$ 50 kHz,

which might normally be expected to move the TAE from the gap to strong continuum interactions, yet no significant change is seen in the mode evolution.

The NOVA calculation of the eigenmodes is linear and these eigenmodes need to be scaled with the experimental measurements to be used in the ORBIT code. The process determines the absolute mode

Fig. 6. Solid curves are simulated reflectometer response, points are reflectometer data, inset are NOVA poloidal harmonics for, a) n=1 mode, b) n=2 mode, c) n=4 mode and d) n=6 mode.

amplitude by simulating the reflectometer response to the eigenmode structure, and scaling the linear eigenmodes to match the absolute reflectometer measurements (which are not a directly local measurement of the mode amplitude) for each of the TAE. Figures 6a - 6d show comparisons of the simulated reflectometer responses (black curves) compared to the experimental measurements. The insets show the dominant poloidal harmonics in Boozer coordinates.

For the n=2 and n=4 modes, the agreement with the shape is reasonable. The measured profiles of the n=1 and n=4 modes have larger amplitude towards the edge than the NOVA simulations, which were found using a conducting boundary at the plasma surface, thus the mode structure near the plasma edge is not well reproduced. However, with a only finite number of poloidal harmonics NOVA cannot in any case resolve the eigenmode structure near the separatrix. Here, the eigenmode radial

Fig. 7. Initial and final beam ion energies for an ORBIT simulation using measured mode amplitude and frequency evolutions.

shapes were fit with only 12 poloidal harmonics. For these reasons, and others, this work

should be viewed as a somewhat qualitative, rather than quantitative, study.
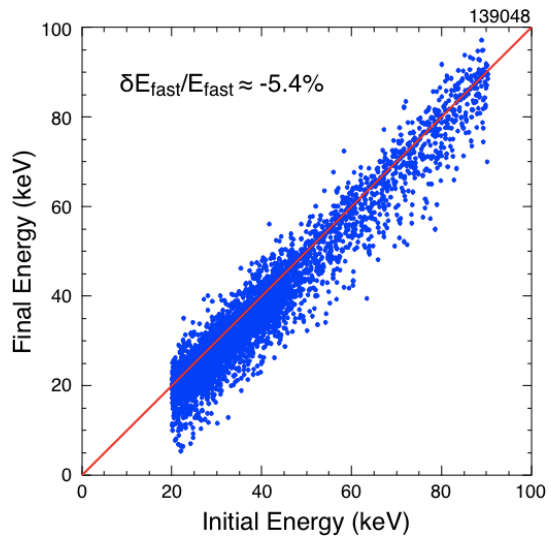
The ORBIT code simulations begin with the growth of the n=2 mode and cover about 2 ms (yellow region, Fig. 4), at which time only the n=1 mode has significant amplitude. In both Figs. 4a and 4b, the frequency and amplitude data is fit with analytic formulas, solid curves, which are used in the ORBIT code simulations described below.

An important effect of the TAE avalanche in the ORBIT simulation is to reduce the net energy of confined beam-ions by $\approx 5.4\%$, as shown in Fig. 7. Each blue point represents a beam ion in the ORBIT simulation; those points near the red line have nearly

Fig. 8. Total neutron rate drop vs. scaled TAE amplitude (red squares), for the confined fast ion population (green diamonds) and due only to fast ion losses (blue circles).

the same initial and final energy (although the energy could have changed through the simulation). At the measured mode amplitude, the fast ions are scattered by $\approx \pm 10$ keV, with a net loss of fast ion energy of $\approx 5.4\%$. Approximately 3% of the fast ions are lost in the simulation using the experimental mode amplitudes.

The change in neutron rate is estimated for the perturbed fast ion distribution using the energy-dependence of the fusion cross-section, together with the drop in fusion rate from redistribution of beam-ions to lower density plasma regions and beam-ion losses. There is a net estimated drop in the neutron rate of $\approx 23\%$, larger than the measured drop of $\approx 12\%$ for the ORBIT simulations using the measured mode amplitude. The scaling of the beam-target neutron rate drop with TAE amplitude is shown in Fig. 8. Simulations are done with nominal, measured mode amplitudes, and with all amplitudes scaled by a factor ranging from 0.1 to 2.5. Up to the measured mode amplitude (normalized mode amplitude of one), the neutron drop is primarily from the loss of energy from the fast ions. Above that amplitude, the losses of fast ions become the dominant mechanism for the drop in neutron rate. The experimental neutron rate drop of $\approx 12\%$ is seen at ≈ 0.7 times the measured mode amplitude.

The change in neutron rate between the initial and final fast ion distributions is calculated separately for the beam-beam and beam-target neutron contributions. The beam-
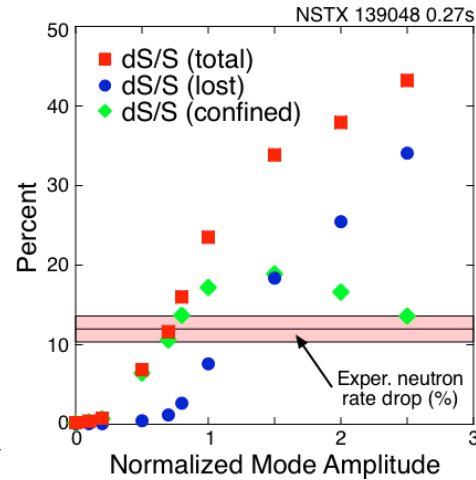
target fusion rate is proportional to $n_{ion}n_b\sigma(E_b)v_b$ where n_{ion} and n_b are the local thermal and beam deuterium densities, σ is the energy-dependent fusion cross-section, and E_b and v_b are the energy and velocity of the beam ion, respectively. Then, taking the fast ion distribution in ORBIT as representative, the beam-target neutron rate will be proportional to

$$S^{B-T} \approx \sum_{i=1}^{N} n_{ion}(\psi_i)\sigma(E_i)v_i$$

where the sum is over the sample fast ion distribution used in ORBIT and $n_{ion}(\psi_i)$ is the thermal deuterium ion density near each beam ion. The sum is done for the initial fast ion distribution, $S^{Initial}$, and the final fast ion distribution, S^{Final}, where S^{Final} also includes the drop in neutron rate from beam ions that were lost. These are not absolute neutron rates, so the relative change is reported as $\delta S^{B-T}/S^{B-T} \approx (S^{Initial}-S^{Final})/S^{Initial}$.

Estimating the neutron rate drop for beam-beam reactions is more difficult. Determining the effective fusion cross-section in the rest frame of one of the fast ions is complicated. However, for a Maxwellian distribution of energetic Deuterium ions, with a temperature of 50 keV, the energy dependence of the fusion rate is approximately linear with temperature [61]. While the beam ion slowing down distribution is neither Maxwellian, nor isotropic, a linear dependence on energy may not be an unreasonable approximation for the fusion cross-section energy dependence. The beam-beam fusion rate is then roughly proportional to $n_b n_b E_b v_b$ and the beam-beam fusion rate is then proportional to

$$S^{B-B} \approx \sum_{i=1}^{N} n_b(\psi_i)E_i v_i$$

and the change is calculated, as for the beam-target rate above, as $\delta S^{B-B}/S^{B-B} \approx (S^{Initial}-S^{Final})/S^{Initial}$. In this shot, TRANSP calculations find that 25% of the neutron rate is from beam-beam reactions, 75% from beam-target and the numbers in Fig. 8 are so weighted.

Taking the experimental values for the mode amplitude, the peak energy in the Alfvén waves comes to about 0.66% of the energy stored in the fast ion population. Based on the ORBIT simulations, a neutron rate drop of 12% corresponds to about 3.6% loss of fast ion energy (and 0.6% of fast ions lost). Thus, we estimate that roughly five to six times as much

energy flowed through the TAE as was present in the waves at peak amplitude. This estimate will be shown to be consistent with the experimentally estimated damping rate, as discussed below. The energy presumably flowed through the TAE and from there to the thermal plasma. If ion Landau damping is much larger than continuum or electron collisional damping, this could provide a mechanism for "alpha-channeling" of fusion-alpha energy [62] to the thermal ions in a reactor. However, even for these relatively large modes the fraction of beam power estimated to be moving through the TAE is very small, << 1%.
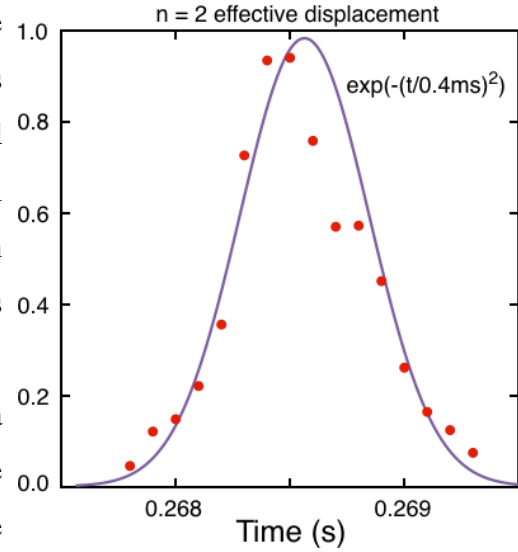

Fig. 9. Experimental n=2 mode amplitude from reflectometer array (red points), Gaussian approximation (solid line)

The energy in the wave is estimated as twice the magnetic fluctuation energy, and the magnetic fluctuation energy is estimated as twice the radial magnetic fluctuation energy (to account for the energy in the poloidal magnetic field fluctuations). Thus, normalized to the magnetic field energy, $\beta_{wave} \approx 4\ (\delta B_r/B)^2$. The peak wave field β_{wave}, volume averaged, is $\approx <4(\delta B_r/B)^2>_{vol} \approx 1.9 \times 10^{-4}$. The fast ion beta is 0.029, and the change in fast ion beta, $\delta\beta_{fast} \approx 1.0 \times 10^{-3}$. Thus, roughly 5.5 times as much energy was lost from the fast ions as was present at peak amplitude in the mode.

The ratio of the peak energy in a wave burst to energy lost to damping can be estimated analytically. The amplitude evolution of the burst can very roughly be fit with a Gaussian shape in time, as shown in Fig.9. The energy lost through damping can then be estimated from the integral of wave energy times the damping rate over the burst.

$$W_{loss}/W_{peak} = 2\gamma_{damp} \int_{-t_0/2}^{t_0/2} \exp\left(-2(t/t_w)^2\right)dt \approx 2\gamma_{damp} \int_{-\infty}^{\infty} \exp\left(-2(t/t_w)^2\right)dt = \gamma_{damp} t_w \sqrt{2\pi}$$

Here, τ_w is the effective width of the TAE burst, and γ_{damp} is the linear damping rate. The damping rate can be estimated by fitting the mode decay rate, which would tend to underestimate the actual damping rate as some drive may still be present. A fit gives an an damping rate of $\gamma_{damp} > 3.8$/ms. Alternatively, a Gaussian amplitude evolution for a burst can be modeled with a constant damping rate and a linearly decreasing drive term over the

period of the burst. Over a period from $-t_0/2 \le t \le t_0/2$, where $t_0 \approx 1.6$ ms, the growth rate can be modeled as:

$$\gamma(t) = \gamma_{drive} - \gamma_{damp} = (\gamma_{damp} - 2\gamma_{damp} t/t_0) - \gamma_{damp} = -2\gamma_{damp} t/t_0$$

The mode amplitude evolution is then:

$$A(t) = \exp\left(\int_{-t_0/2}^{t_0/2} -2\gamma_{damp}(t/t_0)dt\right) = \exp\left(-\gamma_{damp} t_0 (t/t_0)^2\right)$$

The damping rate can then be found by comparing to the Gaussian fit shown in Fig. 9, from which we find $\gamma_{damp} \approx 10$/ms, or $\gamma_{damp}/\omega \approx 1.6\%$. (This is somewhat less than the NOVA estimate of the $n = 2$ mode ion Landau damping of $\gamma_{ion}/\omega \approx 2.1\%$, and including electron collisional and radiative damping would increase this estimate.) Using the empirically determined damping rate, the ratio $W_{loss}/W_{peak} \approx 2$ to 5, so the energy lost from the fast ion population in the ORBIT simulations is in qualitative agreement with the experimental estimates for mode amplitude evolution and damping.

Avalanches in L-mode plasmas

A previous study of fast ion losses from TAE avalanches in L-mode plasmas was described in Ref. ?. The avalanche data was revisited using the updated ORBIT code and analysis techniques employed in the above work. One of the L-mode TAE avalanches is seen in the spectrogram of magnetic fluctuations shown in Fig. 10a. The dominant mode in this case was an $n = 3$ TAE (green contour). There were also weaker $n = 2$, 4 and 6 TAE in the avalanche burst. The burst itself was only ≈ 1ms in duration, shorter than the H-mode case. The drop in the neutron rate was comparable at $\approx 12\%$ (Fig. 10b). The D-alpha data suggests fast ions were lost as in the H-mode case (Fig. 10c).
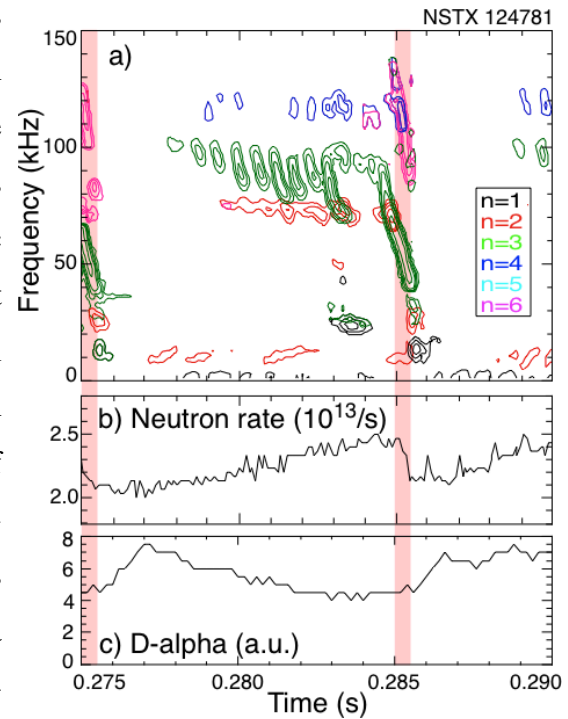
The original choice to study TAE

Fig. 10. a) Spectrogram of magnetic fluctuations showing two TAE avalanche bursts, b) neutron rate drops at each burst, c) Dα spikes at bursts.
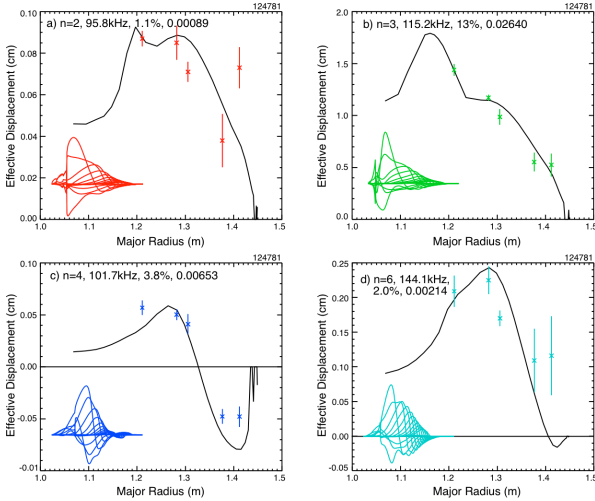
Fig. 11 Solid curves are simulated reflectometer response, points are reflectometer data, inset are NOVA poloidal harmonics for, a) n=2 mode, b) n=3 mode, c) n=4 mode and d) n=6 mode.

avalanches in L-mode plasmas was made to optimize the reflectometer measurements of the mode structure. Producing TAE avalanches in L-mode requires lower voltage neutral beams, for reasons not understood at this time. A Helium pre-fill and gas puffing were used to suppress the H-mode transition. Both the helium content of the plasma and the reduced beam voltage led to a significantly lower neutron rate in the L-mode case.

Previously, the reflectometer data was modeled using only the displacement contribution to the density perturbation. The compressional contribution was approximately modeled by scaling the displacement density perturbation. Here, the reflectometer data has been modeled explicitly using the compressional and displacement terms, which results in only modest changes to the mode amplitudes used in ORBIT. The fits are generally better than in the H-mode case (Fig. 11). Both NOVA and the experimental measurements suggest that the TAE were more core localized than in the H-mode. The $n = 6$ mode has also been included, although the impact of that was modest. The new fits to the reflectometer array data are shown in Fig. 11.

The largest change in the new analysis is that ORBIT has a more accurate calculation of the electric field from the TAE near the rational surfaces. With the more accurate representation of the electric field, fewer fast ion losses are seen in the simulations. However, the reduction in the simulated neutron rate is largely compensated by the recognition of neutron rate drop due to energy loss. In Fig. 13 are shown the net neutron
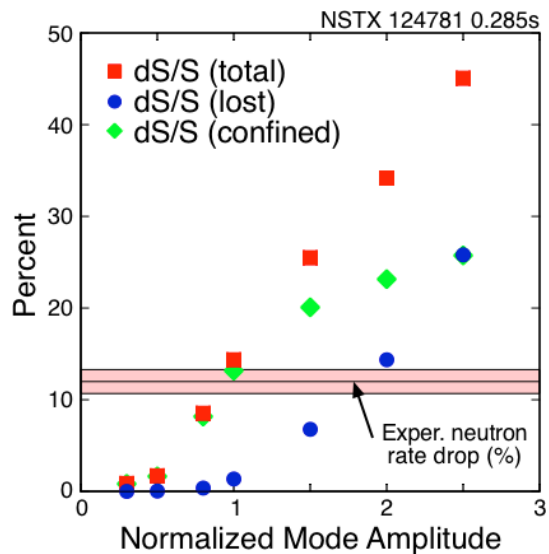

Fig. 12. Simulated neutron rate drop due to TAE avalanche (red), neutron rate drop resulting from lost beam ions (blue) and neutron rate drop in confined beam ion population from energy loss (green).

11

rate drop in ORBIT simulations (red squares), the neutron drop due to lost beam ions (blue squares) and neutron drop in the confined beam ion population due to loss of energy to the TAE. As above, the change in neutron rates are calculated for beam-target and beam-beam neutrons, and those two calculations are combined using the TRANSP partition of $\approx 63\%$ of the neutron rate is from beam-beam reactions and only $\approx 37\%$ are beam-target. The lower beam-target neutron rate from the reduced beam voltage and nominal He target plasma results in a larger percentage of beam-beam neutrons.

As was the case in the H-mode avalanches analyzed above, there is an apparent threshold for energy loss in the fast ion population at about one half the amplitude threshold for fast ion losses. In this example, there is good agreement between the measured neutron rate drop and that predicted at the measured mode amplitude.

Summary and discussion

Simulations of fast ion transport due to TAE avalanches in NSTX are in qualitative agreement with experimental data. A surprising result is that ORBIT simulations predict small fast ion losses up to the measured mode amplitudes, however the energy taken from the fast ions by the TAE is sufficient to reduce the neutron rate as experimentally observed. The perturbation to the beam-target neutron rate is estimated using the change to the fast ion distribution function and the beam-target fusion cross-section and target deuterium density. The calculation of the change to the beam-beam rate is more complicated, so a simple estimate is made based on the change in the effective temperature (energy) in the slowing-down distribution. The scaling and magnitude of the beam-beam and beam-target rate changes are found to be roughly comparable, and the sum is in qualitative agreement with the measured neutron rate change.

The simulations of the new TAE H-mode avalanches were done with a version of ORBIT where the potential fluctuations from the mode near rational surfaces were more accurately calculated. Application of ORBIT with the improved potential fluctuation calculation, and some refinements in the input of mode structure to ORBIT, found a different result than the previous analysis. Then, fast ion losses alone were sufficient to

explain the observed neutron drop. The analysis with the improved calculation of the electric field finds very low levels of fast ion loss at observed mode amplitudes in the previously studied L-mode, but the loss of fast ion energy is sufficient to account for the observed neutron drop.

The simulations of the TAE avalanches in the L-mode case are in good agreement with experiment. However, in the H-mode case the mode amplitudes needed reduction by ≈ 0.7 to get agreement with the observed neutron rate drop. At some level it is surprising the agreement is as good as it is. The use of the ideal eigenmodes, with unphysical interactions with the continuum, the use of the unperturbed fast ion distributions in the presence of multiple Alfvénic instabilities, the use of a guiding center code in a situation with large larmor radii and general uncertainties in equilibrium reconstruction could all potentially contribute to large uncertainty in the simulations. Future experiments with improved diagnostics and more advanced analysis codes will continue to investigate our understanding of fast ion confinement.

Bibliography

[1]   M. Ono, S.M. Kaye, Y.-K.M. Peng, G. Barnes, W. Blanchard, M.D. Carter, J. Chrzanowski, L. Dudek, R. Ewig, D. Gates, R.E. Hatcher, T. Jarboe, S.C. Jardin, D. Johnson, R. Kaita, M. Kalish, C.E. Kessel, H.W. Kugel, R. Maingi, R. Majeski, J. Manickam, B. McCormack, J. Menard, D. Mueller, B.A. Nelson, B.E. Nelson, C. Neumeyer, G. Oliaro, F. Paoletti, R. Parsells, E. Perry, N. Pomphrey, S. Ramakrishnan, R. Raman, G. Rewoldt, J. Robinson, A.L. Roquemore, P. Ryan, S. Sabbagh, D. Swain, E.J. Synakowski, M. Viola, M. Williams, J.R. Wilson and the NSTX Team, Nucl. Fusion **40** (2000) 557.

[2]   R B White, R J Goldston, K M McGuire, et al, Phys. Fluids **26** (1983) 2958.[]   R B White, R J Goldston, K M McGuire, et al, Phys. Fluids **26** (1983) 2958.

[3]   R Kaita, R B White, A W Morris, E D Fredrickson, K M McGuire, S S Medley, T J Murphy, and S D Scott, Phys. Fluids **B 2** 1584 (1990).

[4]   *Beam-driven chirping instability in DIII-D* W W Heidbrink, Plasma Phys. Control. Fusion **37** (1995) 937.

[5]   "*Bounce precession fishbones in the National Spherical Torus Experiment*" E D Fredrickson, L Chen, R B White, Nucl. Fusion **43** (2003) 1258.

[6]   *Measurements of Prompt and MHD-Induced Fast Ion Loss from National Spherical Torus Experiment Plasma* D. S. Darrow, S. S. Medley, A. L. Roquemore, W. W. Heidbrink, A. Alekseyev, F. E. Cecil, J. Egedal, V.Ya.Goloborod'ko, N. N. Gorelenkov, M. Isobe, S. Kaye, M. Miah, F. Paoletti, M. H. Redi, S.N.Reznik, A. Rosenberg, R. White, D. Wyatt, V. A. Yavorskij, in *19th IAEA Fusion Energy Conference, Lyon, France, 14-19 Oct 2002* (IAEA, Vienna)

[7]   Ya. I Kolesnichenko, VS Marchenko and R B White, Phys. Plasmas **13**, 052504 (2006)

[8]   *Fast ion loss in a "sea-of-TAE"*, E.D. Fredrickson, N N Gorelenkov, R E Bell, J E Menard, A L Roquemore, S. Kubota, N A Crocker, W Peebles, Nucl. Fusion **46** (2006) s926.

[9]   *Three-Wave Interactions between Fast-Ion Modes in the National Spherical Torus Experiment*, N. A. Crocker, W. A. Peebles, S. Kubota, E. D. Fredrickson, S. M. Kaye, B. P. LeBlanc, J. E. Menard, Phys. Rev. Lett. **97** (2006) 045002.

[10]   *Experimental studies on fast-ion transport by Alfvén wave avalanches on the National Spherical Torus Experiment*, M. Podestà, W. W. Heidbrink, D. Liu, E. Ruskov, R. E. Bell, D. S. Darrow, E. D. Fredrickson, N. N. Gorelenkov, G. J. Kramer, B. P. LeBlanc, S. S. Medley, A. L. Roquemore, N. A. Crocker, S. Kubota, and H. Yuh, Phys. of Plasmas **16** (2009) p056104.

[11]   *Effects of toroidal rotation shear on toroidicity-induced Alfvén eigenmodes in the National Spherical Torus Experiment*, M. Podestà, R. E. Bell, E. D. Fredrickson, N. N. Gorelenkov, B. P. LeBlanc, W. W. Heidbrink, N. A. Crocker, S. Kubota, and H. Yuh, Phys. of Plasmas **17** (2010) p122501.

[12]   *Non-linear dynamics of toroidicity-induced Alfvén eigenmodes on the National Spherical Torus Experiment*, M. Podestá, R.E. Bell, N.A. Crocker, E.D. Fredrickson, N.N. Gorelenkov, W.W. Heidbrink, S. Kubota, B.P. LeBlanc and H. Yuh, Nucl. Fusion **51** (2011) 063035.

[13]   N.N. Gorelenkov, C.Z. Cheng, Phys. Plasmas **2** (1995) 1961.

[14] E.D. Fredrickson, N. Gorelenkov, C.Z. Cheng, R. Bell, D. Darrow, D. Johnson, S. Kaye, B. LeBlanc, J. Menard, S. Kubota, W. Peebles, Phys. Rev. Lett. **87**, (2001) 145001.

[15] *Compressional Alfven Eigenmode Dispersion in Low Aspect Ratio plasmas*, N N Gorelenkov, C Z Cheng, E Fredrickson, Phys. Plasmas **9** (2002) 3483.

[16] E D Fredrickson, N N Gorelenkov, C Z Cheng, R. Bell, D. Darrow, D. Gates, D. Johnson, S. Kaye, B. LeBlanc, D. McCune, J. Menard, S. Kubota, W. Peebles, Phys. of Plasmas **9** (2002) 2069.

[17] *Compressional Alfvén eigenmode instability in NSTX*, N N Gorelenkov, C Z Cheng, E Fredrickson, E Belova, D Gates, S Kaye, G J Kramer, R Nazikian, R B White, Nucl. Fusion **42** (2002) 977.

[18] *N N Gorelenkov, E Fredrickson, E Belova, C Z Cheng, D Gates, S Kaye, R B White*, in 19th IAEA Fusion Energy Conference, Lyon, France, 14-19 Oct 2002 (IAEA, Vienna) paper IAEA-CN-94/TH/7-1 Ra

[19] *Theory and Observations of High Frequency Alfvén Eigenmodes in Low Aspect Ratio Plasmas*, N.N. Gorelenkov, E. Fredrickson, E. Belova, C.Z. Cheng, D. Gates, S. Kaye, and R. White, Nucl. Fusion, **43** (2003) 228.

[20] *Numerical Study of Instabilities Driven by Energetic Neutral Beam Ions in NSTX*, E Belova, N N Gorelenkov, C Z Cheng, E D Fredrickson, in Proceedings of the 30th European Physical Society Conference on Controlled Fusion and Plasma Physics, St. Petersburg, Russia, July 2003, ECA Vol. 27A, P-3.102.

[21] "*Destabilization of fast magnetoacoustic waves by circulating energetic ions in toroidal plasmas*", V. S. Belikov and Ya. I. Kolesnichenko, R. B. White, Phys. of Plasmas **10** (2003) 4771.

[22] "*Phenomenology of compressional Alfvén eigenmodes*", E. D. Fredrickson, N. N. Gorelekov and J. Menard, Phys. of Plasmas **11** (2004) 3653.

[23] "*Discrete compressional Alfvén eigenmode spectrum in tokamaks*", Gorelenkov N N, Fredrickson E D, Heidbrink W W, Crocker N A, Kubota S and Peebles W A, Nucl. Fusion **46** (2006) S933.

[24] *Observation of compressional Alfvén eigenmodes (CAE) in a conventional tokamak*, W W Heidbrink, E D Fredrickson, N N Gorelenkov, T L Rhodes, M A Van Zeeland, Nucl. Fusion **46** (2006) 324.

[25] "*High-frequency shear Alfvén instability driven by circulating energetic ions in NSTX*" Ya. Kolesnichenko, R B White, Yu. V Yakovenko, Phys.of Plasmas **13** (2006) 122503,

[26]   *"Interpretation of Mode Frequency Sweeping in JET and NSTX"*, H. L. Berk, C. J. Boswell, D. Borba , B. N. Breizman, A. C. A. Figueiredo, E. D. Fredrickson, N. N. Gorelenkov, R. W. Harvey, W. W. Heidbrink, T. Johnson, S. S. Medley, M. F. F. Nave, S. D. Pinches, E. Ruskov, S. E. Sharapov, and JET EFDA contributors, in proceedings of the 21st IAEA Fusion Energy Conference. 16 - 21 October 2006, Chengdu, China (IAEA, Vienna, 2007) paper IAEA-TH/3-1

[27]   *Numerical Modeling of NBI-driven GAE modes*, Belova, E. V., Gorelenkov, N. N., Fredrickson, E. D., Bull. American Physical Society, 2009 APS April Meeting, abstract #S1.070 (2009).

[28]   *"Physics of energetic particle-driven instabilities in the START spherical tokamak "*, McClements K G, Gryaznevich M P, Sharapov S E, Akers R J, Appel L C, Counsell G F, Roach C M and Majeski R 1999 Plasma Phys. Control. Fusion **41** 661.

[29]   *Frequency sweeping Alfvén instabilities driven by super-Alfvénic beams in the spherical tokamak START*, M P Gryaznevich and S E Sharapov, Nuclear Fusion **40** (2000) 907.

[30]   *"Observation of CAEs on MAST"* Appel L C, Akers R J, Martin R and Pinfold T, 2004 31st EPS Conf. on Plasma Physics (London, UK) vol 28G P-4.198 (Monotypia Franchi, Ciita` di Catelo, Perugia)

[31]   *"Spectroscopic determination of the internal amplitude of frequency sweeping TAE"*, S D Pinches, H L Berk, M P Gryaznevich, S E Sharapov, Plasma Phys. and Cont. Fusion **46** (2004) s47.

[32]   *Experimental studies of instabilities and confinement of energetic particles on JET and MAST*, Sharapov, S.E., Alper, B., Andersson, F., Baranov, Yu.F., Berk, H.L., Bertalot, L., Borba, D., Boswell, C., Breizman, B.N., Buttery, R., Challis, C.D., de Baar, M., de Vries, P., Eriksson, L.-G., Fasoli, A., Galvao, R., Goloborod'ko, V., Gryaznevich, M.P., Hastie, R.J., Hawkes, N.C., Helander, P., Kiptily, V.G., Kramer, G.J., Lomas, P.J., Mailloux, J., Mantsinen, M.J., Martin, R., Nabais, F., Nave, M.F., Nazikian, R., Noterdaeme, J.-M., Pekker, M.S., Pinches, S.D., Pinfold, T., Popovichev, S.V., Sandquist, P., Stork, D., Testa, D., Tuccillo, A., Voitsekhovich, I., Yavorskij, V., Young, N.P., Zonca, F., Nuclear Fusion **45**, (2005) 1168.

[33]   *Alfven eigenmodes in spherical Tokamaks*, Gryaznevich, M.P.; Sharapov, S.E.; Berk, H.L.; Pinches, S.D., Transactions of the Institute of Electrical Engineers of Japan, Part A 2005, vol.125-A, pp. 908-13

[34] *Theoretical interpretation of frequency sweeping observations in the Mega-Amp Spherical Tokamak*, R. G. L. Vann , R. O. Dendy, M. P. Gryaznevich, Phys. Plasmas **12** (2005) 032501

[35] *Anisotropic fast neutral particle spectra in the MAST spherical tokamak*, M.R. Tournianski, R J Akers, P G Carolan, and D L Keeling, Plasma Physics and Cont. Fusion **47** (2005) 671.

[36] "*Perturbative and non-perturbative modes in START and MAST* ", Gryaznevich M P and Sharapov S E 2006 Nucl. Fusion **46** S942

[37] "*Modelling of beam-driven high frequency Alfvén eigenmodes in MAST* ", Lilley M K, Sharapov S E, Smith H M, Akers R J, McCune D and MAST team 35th EPS Conf. on Plasma Physics (2008 Crete, Greece)

[38] *Compressional Alfvén Eigenmodes on MAST*, L C Appel, T Fülöp, M J Hole, H M Smith, S D Pinches, R G L Vann and The MAST Team, Plasma Phys. Control. Fusion **50** (2008) 115011.

[39] *Recent experiments on Alfvén eigenmodes in MAST*, M.P. Gryaznevich, S.E. Sharapov, M. Lilley, S.D. Pinches, A.R. Field, D. Howell, D. Keeling, R. Martin, H. Meyer, H. Smith, R. Vann, P. Denner, E. Verwichte and the MAST Team, Nucl. Fusion **48** (2008) 084003.

[40] '*Characteristics of Alfvén eigenmodes, burst modes and chirping modes in the Alfvén frequency range driven by negative ion based neutral beam injection in JT-60U*', Y. Kusama, G.J. Kramer, H. Kimura, M. Saigusa, T. Ozeki, K. Tobita, T. Oikawa, K. Shinohara, T. Kondoh, M. Moriyama, F.V. Tchernychev, M. Nemoto, A. Morioka, M. Iwase, N. Isei, T. Fujita, S. Takeji, M. Kuriyama, Nuclear Fusion, **39** (1999) 1837.

[41] *Investigation of high-n TAE modes excited by minority-ion cyclotron heating in JT-60U*, M Saigusa, h Kimura, S Moriyama, Y Neyatani, T Fujii, Y Koide, T Kondoh, M Sato, M Nemoto, Y Kamada, and JT-60 team, Plasma Phys. Control. Fusion **37** 295 (1995).

[42] *Measurements of the radial structure and poloidal spectra of toroidal Alfvén eigenmodes in the Tokamak Fusion Test Reactor*, R D Durst, R J Fonck, k L Wong, C Z Cheng, E D Fredrickson, S F Paul, Phys. Fluids **B 4** (1992) 3707.

[43] *Alpha-driven magnetohydrodynamics (MHD) and MHD-induced alpha loss in the Tokamak Fusion Test Reactor*, Z. Chang,† R. Nazikian, G.-Y. Fu, R. B. White, S. J. Zweben, E. D. Fredrickson, S. H. Batha,a) M. G. Bell, R. E. Bell, R. V. Budny, C. E. Bush,b) L. Chen,c) C. Z. Cheng, D. Darrow, B. LeBlanc, F. M. Levinton,a) R. P. Majeski, D. K. Mansfield, K. M. McGuire, H. K. Park, G. Rewoldt, E. J. Synakowski, W. M. Tang,

G. Taylor, S. von Goeler, K. L. Wong, L. Zakharov, and the TFTR Group, Phys. Plasmas **4** (1997) 1610.

[44] *An investigation of beam driven Alfvén instabilities in the DIII-D tokamak*, W W Heidbrink, E J Strait, E Doyle, G Sager, R T Snider, Nucl. Fusion **31** (1991) 1635.

[45] *Central flattening of the fast-ion profile in reversed-shear DIII-D discharges*, W.W. Heidbrink M.A. Van Zeeland, M.E. Austin, K.H. Burrell, N.N. Gorelenkov, G.J. Kramer, Y. Luo, M.A. Makowski, G.R. McKee, C. Muscatello, R. Nazikian, E. Ruskov, W.M. Solomon, R.B. White and Y. Zhu, Nucl. Fusion **48** (2008) 084001

[46] *Observation of TAE activity in JET*, S Ali-Arshad and D J Campbell, Plasma Phys. and Control. Fusion **37** 715 (1995).

[47] *MHD Spectroscopy* A Fasoli, D Testa, S Sharapov, H L Berk, B Breizman, A Gondhalekar, R F Heeter, M Mantsinen, Plasma Phys. Control. Fusion **44** (2002) B159–B172

[48] *Fast-ion transport induced by Alfvén eigenmodes in the ASDEX Upgrade tokamak*, M. Garcia-Munoz, I.G.J. Classen, B. Geiger, W.W. Heidbrink, M.A. Van Zeeland, S. Äkäslompolo, R. Bilato, V. Bobkov, M. Brambilla, G.D. Conway, S. da Graça, V. Igochine, Ph. Lauber, N. Luhmann, M. Maraschek, F. Meo, H. Park, M. Schneller, G. Tardini and the ASDEX Upgrade Team, Nucl. Fusion **51** (2011) 103013

[49] *Kinetic Alfvén eigenmodes at ASDEX Upgrade*, Ph Lauber, M Brüdgam, D Curran, V Igochine, K Sassenberg, S Günter, M Maraschek, M García-Muñoz, N Hicks and the ASDEX Upgrade Team, Plasma Phys. Control. Fusion **51** (2009) 124009

[50] *Three-Wave Interactions between Fast-Ion Modes in the National Spherical Torus Experiment*, N. A. Crocker, W. A. Peebles, S. Kubota, E. D. Fredrickson, S. M. Kaye, B. P. LeBlanc, J. E. Menard, Phys. Rev. Lett. **97** (2006) 045002.

[51] *Non-linear dynamics of toroidicity-induced Alfvén eigenmodes on the National Spherical Torus Experiment*, M. Podestá, R.E. Bell, N.A. Crocker, E.D. Fredrickson, N.N. Gorelenkov, W.W. Heidbrink, S. Kubota, B.P. LeBlanc and H. Yuh, Nucl. Fusion **51** (2011) 063035.

[52] *Observation of global Alfvén eigenmode avalanche events on the National Spherical Torus Experiment*, E.D. Fredrickson, N.N. Gorelenkov, E. Belova, N.A. Crocker, S. Kubota, G.J. Kramer, B. LeBlanc, R.E. Bell, M. Podesta, H. Yuh and F. Levinton, Nucl. Fusion **52** (2012) 043001

[53]   *Modeling fast-ion transport during toroidal Alfvén eigenmode avalanches in National Spherical Torus Experiment*, E. D. Fredrickson, N. A. Crocker, R. E. Bell, D. S. Darrow, N. N. Gorelenkov, G. J. Kramer, S. Kubota, F. M. Levinton, D. Liu, S. S. Medley, M. Podestá, K. Tritz, R. B. White, and H. Yuh, Phys. of Plasmas **16** (2009), 122505.

[54]   F.M. Levinton and H. Yuh, Rev. Sci. Instrum. 74 (2008) p 10F522

[55]   '*Transport with reversed shear in the National Spherical Torus Experiment*', F. M. Levinton, H. Yuh, M. G. Bell, R. E. Bell, L. Delgado-Aparicio, M. Finkenthal, E. D. Fredrickson, D. A. Gates, S. M. Kaye, B. P. LeBlanc, R. Maingi, J. E. Menard, D. Mikkelsen, D. Mueller, R. Raman, G. Rewoldt, S. A. Sabbagh, D. Stutman, K. Tritz, and W. Wang, Phys. Plasmas **14**, 056119 (2007).

[56]   R V Budny, Nucl. Fusion **34** (1994) 1247.

[57]   *High spatial sampling global mode structure measurements via multichannel reflectometry in NSTX*, N A Crocker, W A Peebles, S Kubota, J Zhang, R E Bell, E D Fredrickson, N N Gorelenkov, B P LeBlanc, J E Menard, M Podestà, S A Sabbagh, K Tritz and H Yuh, Plasma Phys. Control. Fusion **53** (2011) 105001.

[58]   *Kinetic Extensions of Magnetohydrodynamic Models for Axisymmetric Toroidal Plasmas*, C. Z. Cheng Phys. Reports (A Review Sec. of Phys. Letters.), **211**, 1-51 (February, 1992)

[59]   *Interpretation of core localized Alfvén eigenmodes in DIII-D and Joint European Torus reversed magnetic shear plasmas*, G. J. Kramer, R. Nazikian, B. Alper, M. de Baar, H. L. Berk, G.-Y. Fu, N. N. Gorelenkov, G. McKee, S. D. Pinches, T. L. Rhodes, S. E. Sharapov, W. M. Solomon,M. A. van Zeeland, Phys. Plasmas **13** (2006) 056104.

[60]   R. B. White and M. S. Chance, Phys. Fluids **27**, 2455 (1984).

[61]   J. D. Huba, NRL Plasma Formulary Naval Research Laboratory, Washington DC, 1994, p. 45.

[62]   N.J. Fisch, J-R. Rax, Phys. Rev. Lett. **69** (1992) 612.

[]   *Calculation of the non-inductive current profile in high-performance NSTX plasmas*, S.P. Gerhardt, E. Fredrickson, D. Gates, S. Kaye, J. Menard, M.G. Bell, R.E. Bell, B.P. Le Blanc, H. Kugel, S.A. Sabbagh and H. Yuh, Nucl. Fusion **51** 033004 (2011).